Supporting Information

Nitrogen and Sulfur Co-Doped $Ti_3C_2T_x$ MXene for High-Rate Lithium-Ion Batteries

Renfei Cheng[a,b], Tao Hu[c], Jinxing Yang[a, b], Zuohua Wang[d], Weizhen Wang[a], Yan Liang[a], Zhiqing Yang[a], Hongwang Zhang[d], Xiaohui Wang[a,*]

[a] Shenyang National Laboratory for Materials Science, Institute of Metal Research, Chinese Academy of Sciences, Shenyang 110016, China
[b] School of Materials Science and Engineering, University of Science and Technology of China, Shenyang 110016, China
[c] Institute of Materials Science and Devices, Suzhou University of Science and Technology, Suzhou 215009, China
[d] National Engineering Research Center for Equipment and Technology of Cold Strip Rolling, College of Mechanical Engineering, Yanshan University, Qinhuangdao 066004, China
* Corresponding author,
E-mail address: wang@imr.ac.cn (X.H. Wang)

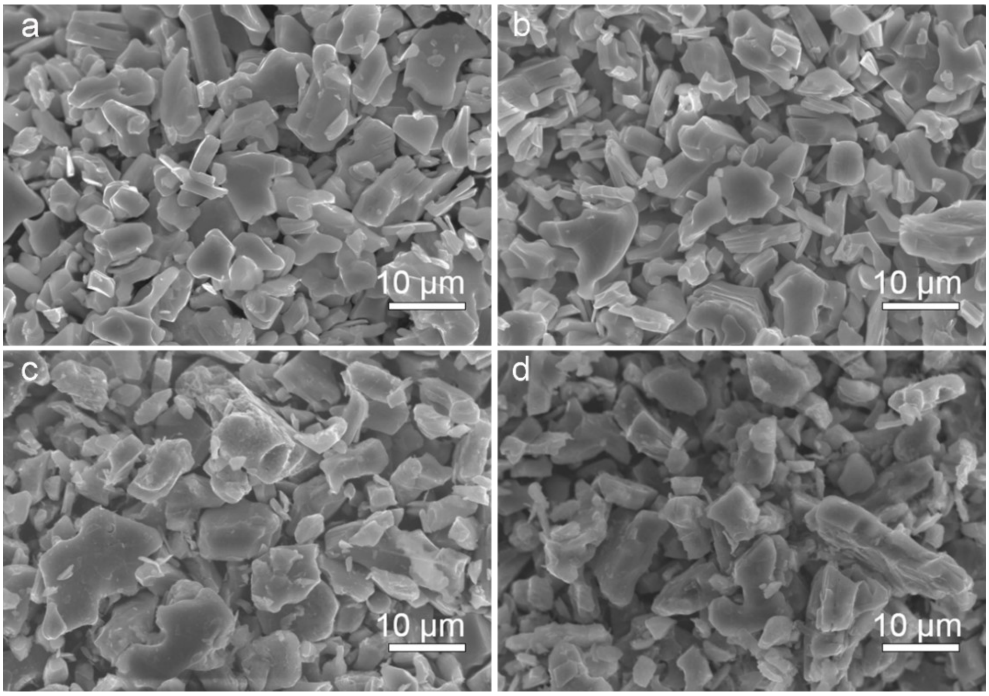

Fig. S1 SEM images of (a) $Ti_3C_2T_x$, (b) N-$Ti_3C_2T_x$, (c) $NS_{0.1}$-$Ti_3C_2T_x$, and (d) $NS_{0.5}$-$Ti_3C_2T_x$.

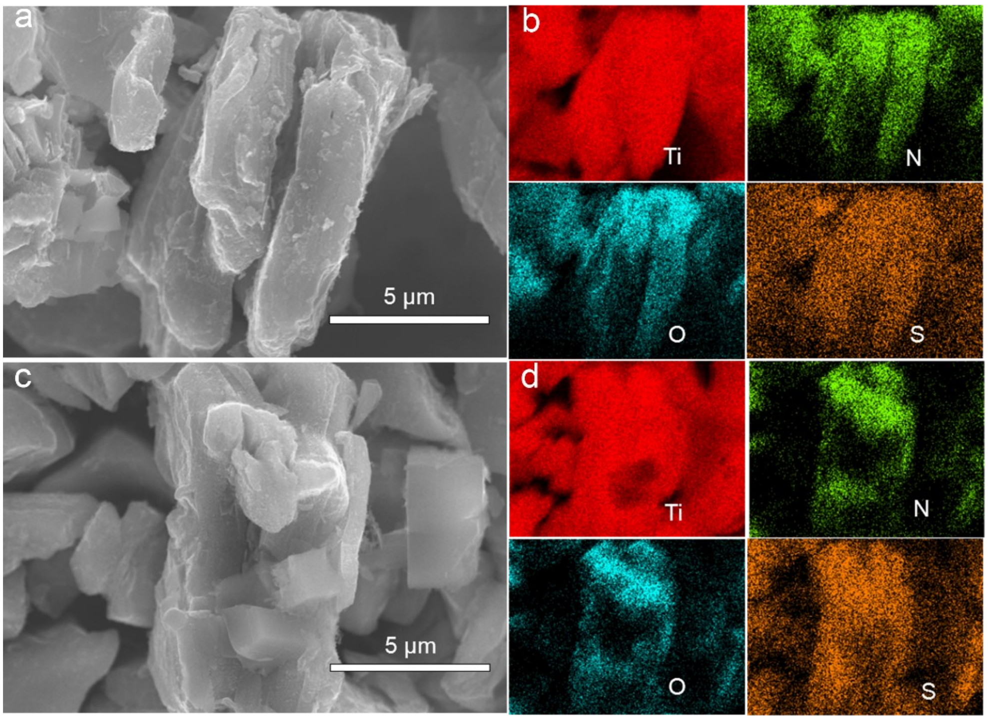

Fig. S2 (a) $NS_{0.1}$-$Ti_3C_2T_x$, corresponding elemental mapping images (b) for the distribution of Ti, N, O and S elements, respectively. (c) $NS_{0.5}$-$Ti_3C_2T_x$, corresponding elemental mapping images (d) for the distribution of Ti, C, O and S elements, respectively.

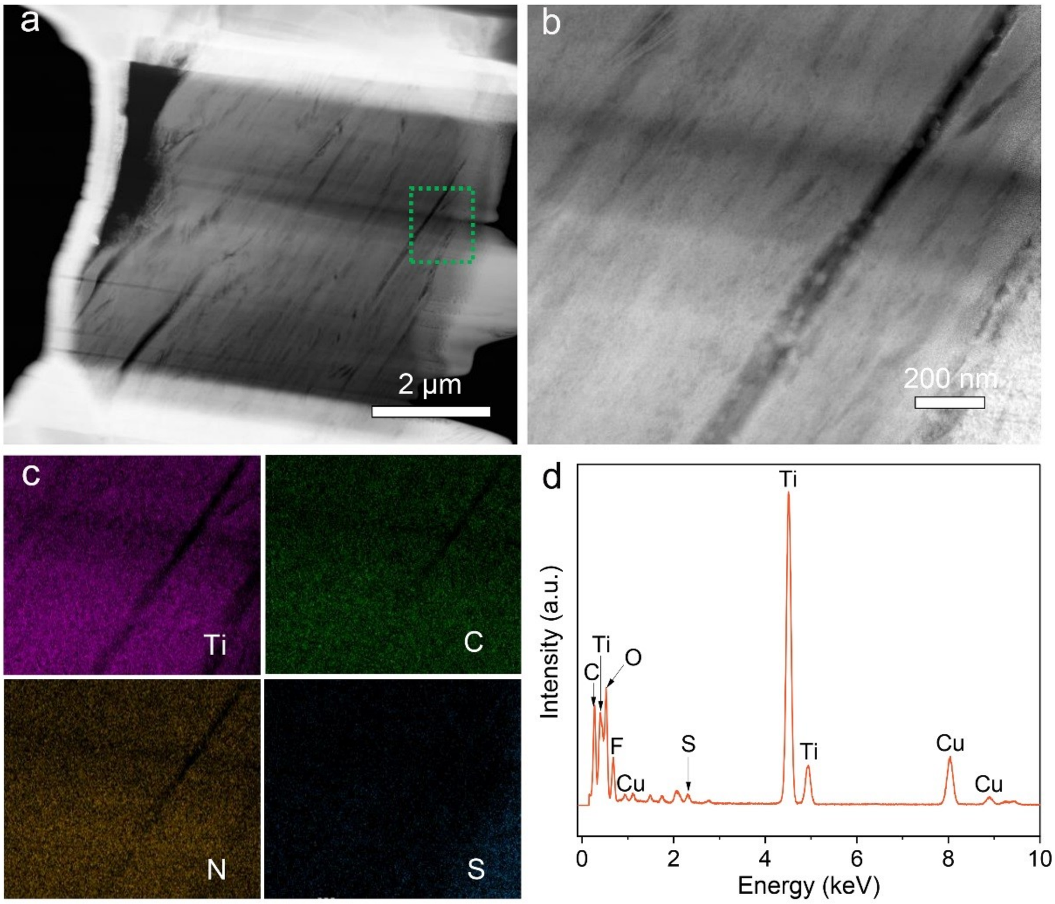

Fig. S3 Typical STEM image and EDS mapping of $NS_{0.3}$-$Ti_3C_2T_x$. (a) Cross sectional microstructure of $NS_{0.3}$-$Ti_3C_2T_x$. (b) HAADF image of marked area by green rectangular and (c) corresponding elemental mappings of Ti, C, N, and S elements. (d) STEM-EDS spectrum of $NS_{0.3}$-$Ti_3C_2T_x$. The atomic ratios of elements are listed in Table S1.

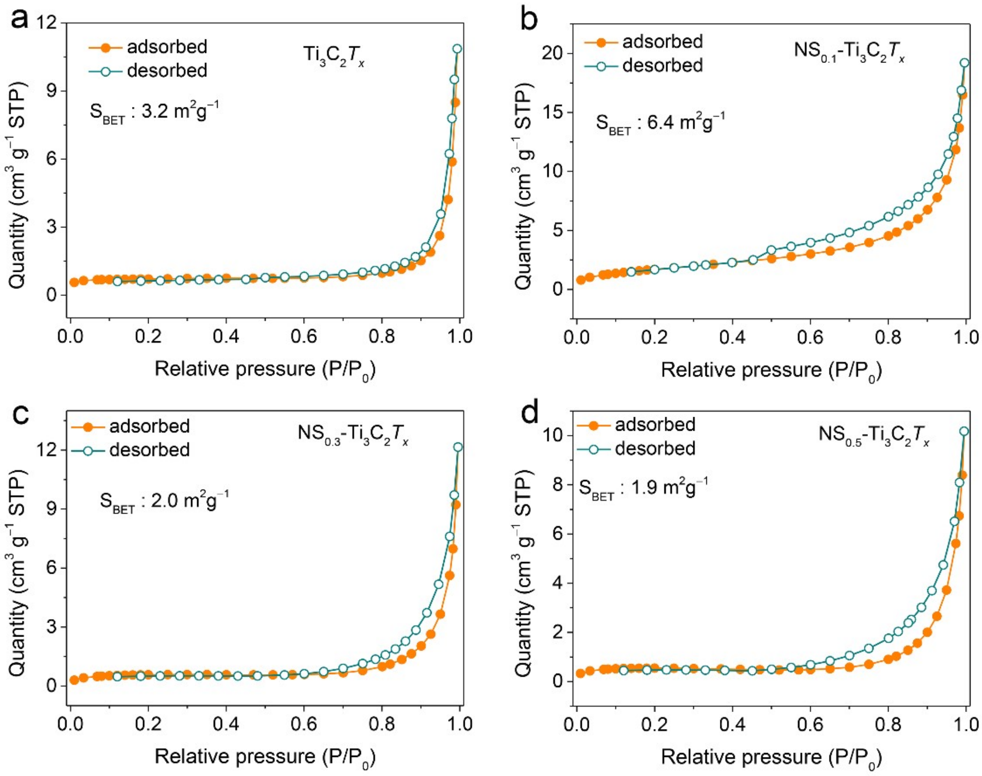

Fig. S4 Nitrogen adsorption/desorption isotherms of (a) pristine $Ti_3C_2T_x$, (b) $NS_{0.1}$–$Ti_3C_2T_x$, (c) $NS_{0.3}$–$Ti_3C_2T_x$ and (d) $NS_{0.5}$–$Ti_3C_2T_x$. The BET specific surface areas of aforementioned samples are 3.2, 6.4, 2.0 and 1.9 m^2 g^{-1}, respectively.

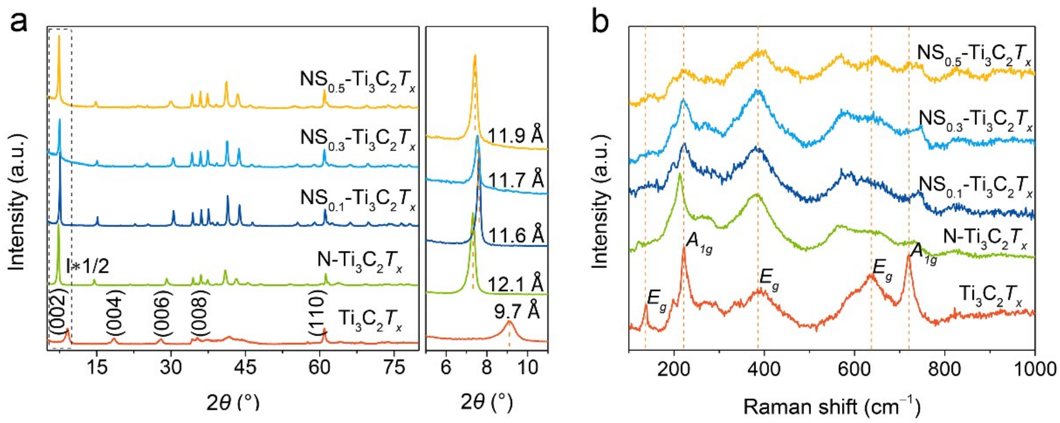

Fig. S5 (a) XRD patterns and (b) Raman spectra of pristine $Ti_3C_2T_x$ and N, S co-doped $Ti_3C_2T_x$.

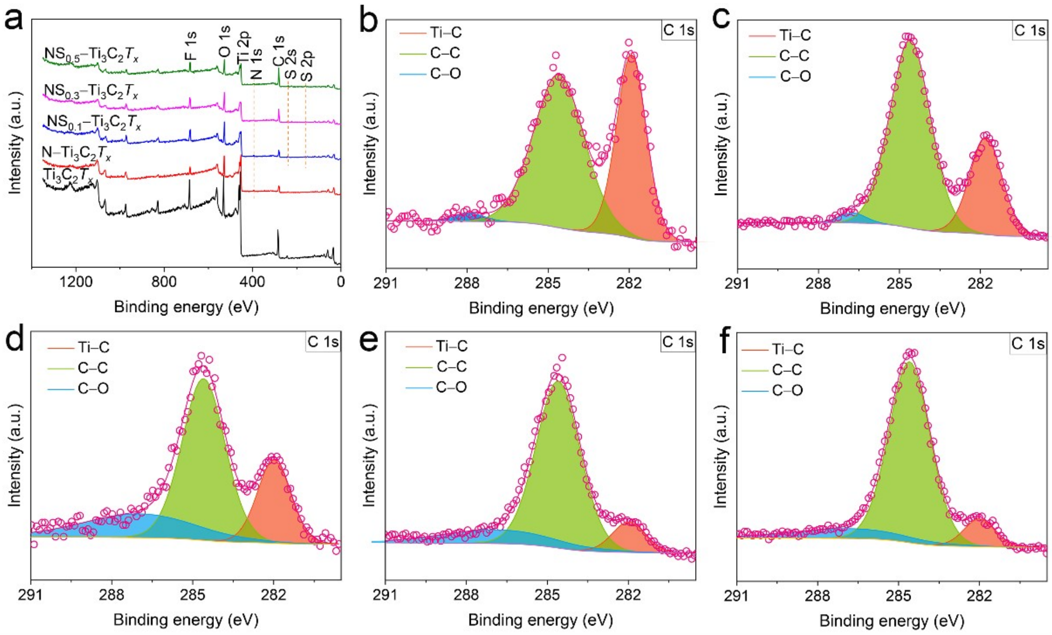

Fig. S6 (a) XPS survey spectra of pristine $Ti_3C_2T_x$, N-$Ti_3C_2T_x$, $NS_{0.1}$-$Ti_3C_2T_x$, $NS_{0.3}$-$Ti_3C_2T_x$, and $NS_{0.5}$-$Ti_3C_2T_x$. High-resolution C 1s XPS spectra of (b) $Ti_3C_2T_x$, (c) N-$Ti_3C_2T_x$, (d) $NS_{0.1}$-$Ti_3C_2T_x$, (e) $NS_{0.3}$-$Ti_3C_2T_x$, and (f) $NS_{0.5}$-$Ti_3C_2T_x$.The XPS spectra were recorded after Ar sputtering for 120 s.

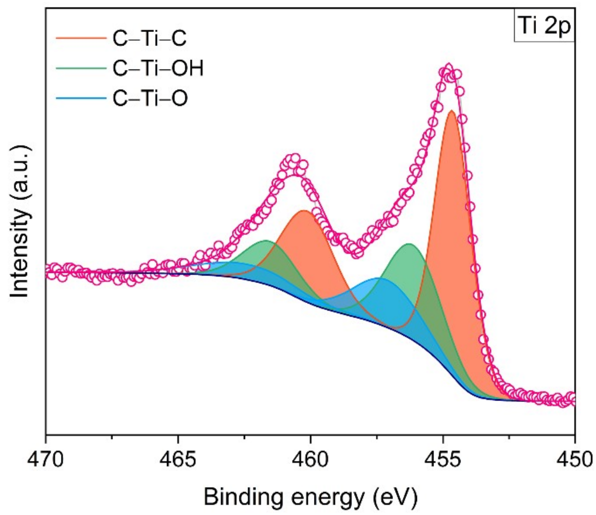

Fig. S7 High-resolution Ti 2p XPS spectra of pristine $Ti_3C_2T_x$. The XPS spectra were recorded after Ar sputtering for 120 s.

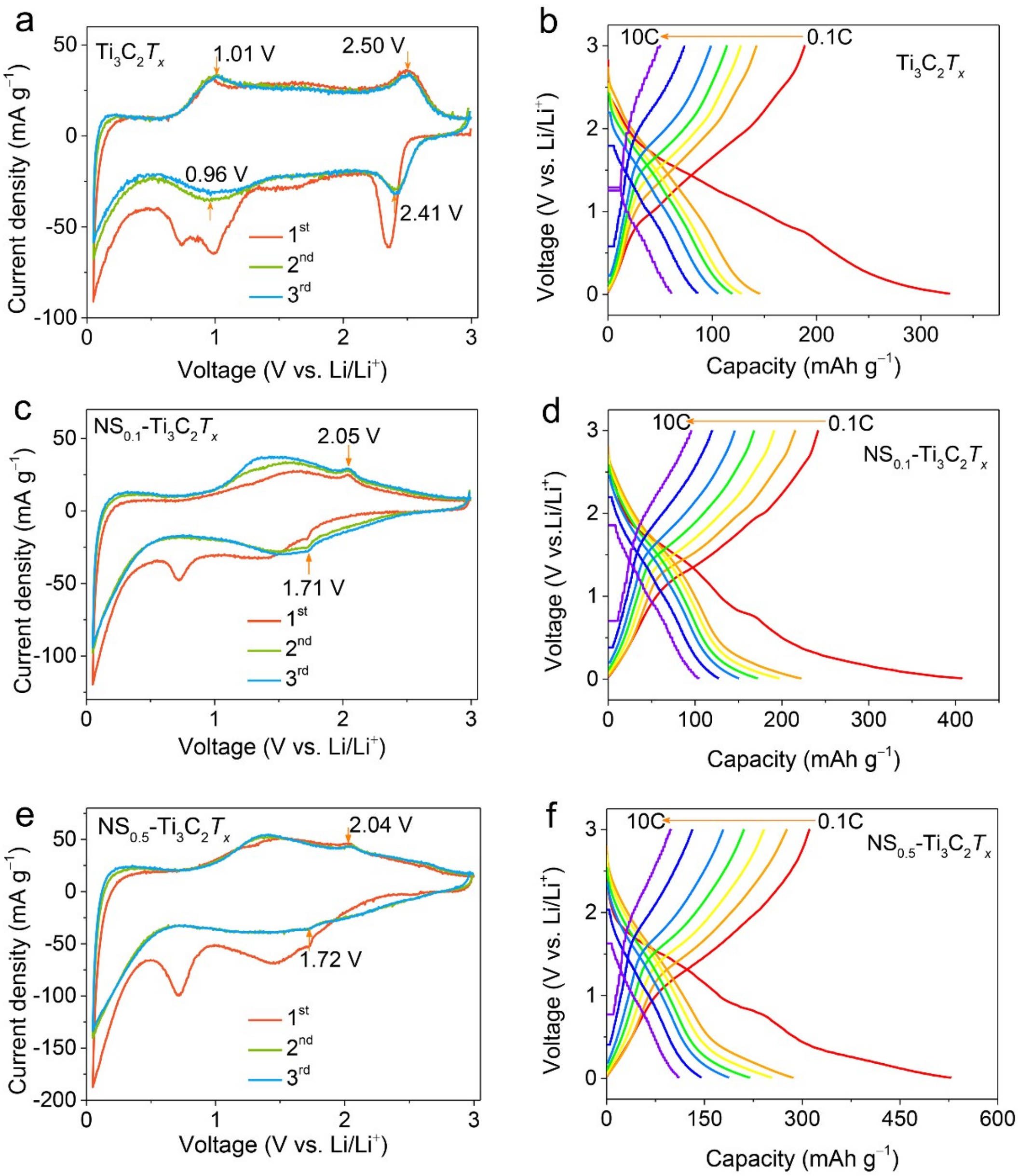

Fig. S8 CV curves of (a) pristine $Ti_3C_2T_x$, (c) $NS_{0.1}$-$Ti_3C_2T_x$, (e) $NS_{0.5}$-$Ti_3C_2T_x$ electrodes. Galvanostatic charge and discharge curves of (b) N-$Ti_3C_2T_x$, (d) $NS_{0.1}$-$Ti_3C_2T_x$ and (f) $NS_{0.5}$-$Ti_3C_2T_x$ cycled at various rates.

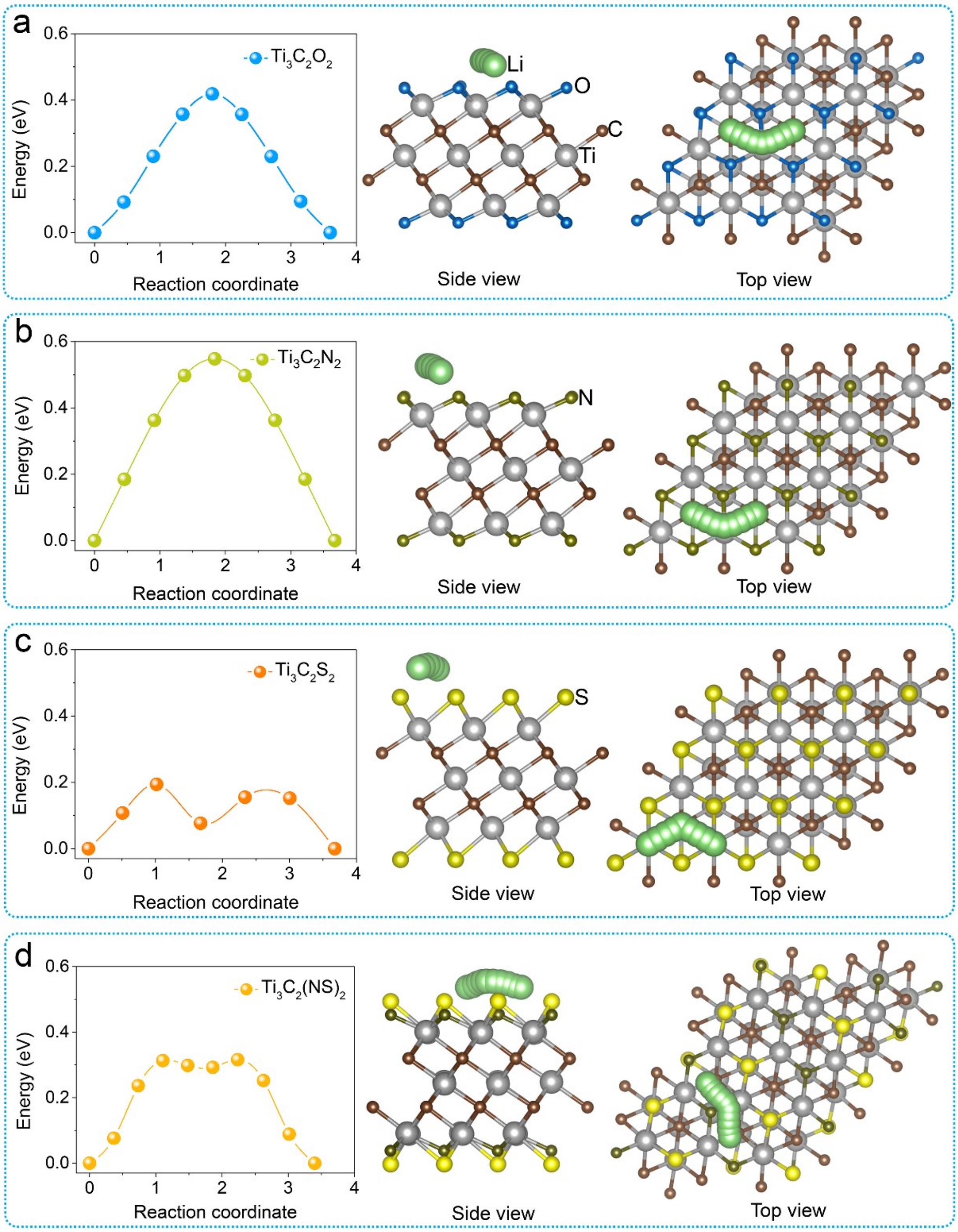

Fig. S9 Diffusion barrier profiles of Li on (a) $Ti_3C_2O_2$, (b) $Ti_3C_2N_2$, (c) $Ti_3C_2S_2$ and (d) $Ti_3C_2(NS)_2$ and the corresponding energetically optimized Li migration pathways from side and top view.

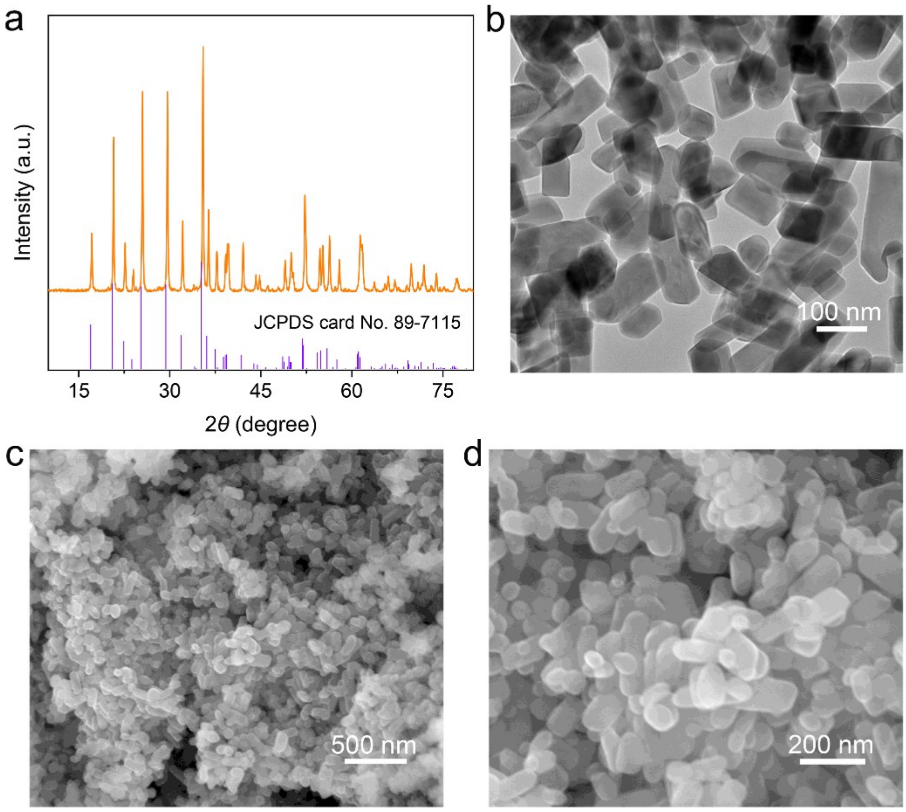

Fig. S10 XRD pattern of the as-prepared $LiMn_{0.5}Fe_{0.5}PO_4$ product. TEM image (b), and SEM images (c, d) of $LiMn_{0.5}Fe_{0.5}PO_4$/C material.

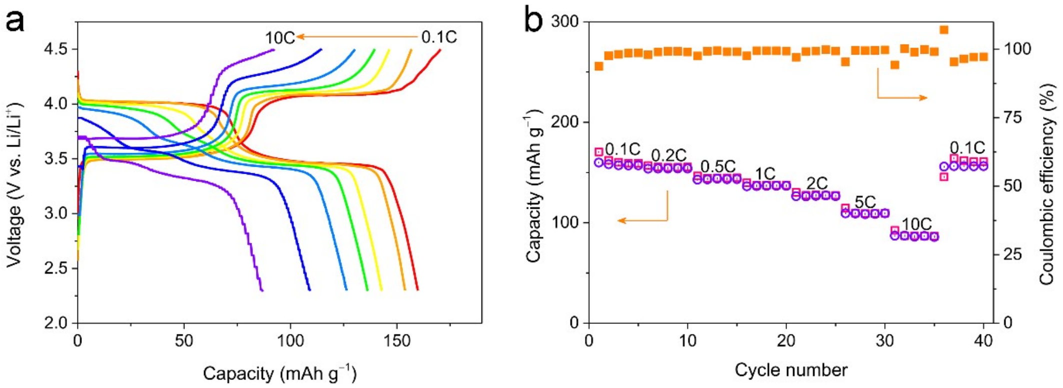

Fig. S11 (a) Typical charge/discharge curves of $LiMn_{0.5}Fe_{0.5}PO_4$/C at current rates ranging from 0.1 to 10C. (b) Rate capability.

Table S1 Summary of atomic ratio in the $NS_{0.3}$–$Ti_3C_2T_x$.

$NS_{0.3}$–$Ti_3C_2T_x$	Element							
	C	O	F	Al	Si	S	Ti	Cu
Subsurface	25.22	13.59	5.02	0.68	0.35	1.11	45.36	8.67
Interior	20.58	11.99	5.16	0.56	0.42	0.70	51.27	9.31

Table S2 Atomic concentration of elements in surface layers of pristine–$Ti_3C_2T_x$, N–$Ti_3C_2T_x$, $NS_{0.1}$–$Ti_3C_2T_x$, $NS_{0.3}$–$Ti_3C_2T_x$, and $NS_{0.5}$–$Ti_3C_2T_x$, samples.

Sample	Element						
	Ti	O	C	F	Al	N	S
pristine–$Ti_3C_2T_x$	19.0	21.3	36.0	14.4	9.3	-	-
N–$Ti_3C_2T_x$	27.2	25.1	32.1	7.4	5.2	3.0	-
$NS_{0.1}$–$Ti_3C_2T_x$	10.9	17.4	52.6	8.2	6.9	2.5	1.5
$NS_{0.3}$–$Ti_3C_2T_x$	12.0	16.7	55.3	7.8	3.4	2.0	2.9
$NS_{0.5}$–$Ti_3C_2T_x$	11.1	15.3	54.2	9.6	3.5	3.5	2.8

Table S3 Ti 2p core level peak analyses of $Ti_3C_2T_x$ MXenes after Ar^+ sputtering 120 s. The Ti 2p core level was fitted with a fixed area ratio of 2:1 for all Ti $2p_{3/2}$–$Ti2p_{1/2}$ and doublet separation of 5.5 eV for C–Ti–C, C–Ti–OH, C–Ti–O, C–Ti–S, C–Ti–N, and C–Ti–ON.

Sample	Fraction / %					
	C–Ti–C 454.9±0.1eV	C–Ti–N 455.5±0.1eV	C–Ti–OH 456.3±0.1eV	C–Ti–S 457.0±0.1eV	C–Ti–O 457.2eV±0.1eV	C–Ti–ON 458.2±0.1eV
pristine–$Ti_3C_2T_x$	53.6	–	28.6	–	17.8	–
N–$Ti_3C_2T_x$	40	5.0	–	–	50	5.0
$NS_{0.1}$–$Ti_3C_2T_x$	42.3	6.3	–	4.2	40.9	6.3
$NS_{0.3}$–$Ti_3C_2T_x$	41.5	1.2	–	5.0	49.8	2.5
$NS_{0.5}$–$Ti_3C_2T_x$	45.2	3.1	–	6.2	42.4	3.1

Table S4. Comparison of the volume expansion for $NS_{0.3}$-$Ti_3C_2T_x$ in our work with widely reported electrode materials.

Samples	Volume expansion (%)	Reference
$NS_{0.3}$-$Ti_3C_2T_x$	0.6	This work
$LiCoO_2$	1.8	Ref.[1]
VPO_4	2.1	Ref.[2]
NCM111	1.2	Ref.[3]
Nb_2CT_x	2.3	Ref.[4]
$LiFePO_4$	6.8	Ref.[5]
VO_2	6.0	Ref.[6]
$LiMn_2O_4$	16	Ref.[7]
$Li_4Ti_5O_{12}$	0.8	Ref.[8]
Graphite	10.7	Ref.[9]
TiO_2	3.7	Ref.[10]

References

1 G. G. Amatucci, J. M. Tarascon, L. C. Klein, *J. Electrochem. Soc.* 1996, **143**, 1114.

2 S. S. Fedotov, A. S. Samarin,; V. A. Nikitina, K. J. Stevenson, A. M. Abakumov, E. V. *ACS Appl. Mater. Interfaces,* 2019, **11**, 12431-12440.

3 A. O. Kondrakov, A. Schmidt, J. Xu, H. Geßwein, R. Mönig, P. Hartmann, H. Sommer, T. Brezesinski, J. Janek, *J. Phys. Chem. C*, 2017, **121**, 3286-3294.

4 R. Cheng, T. Hu, Z. Wang, J. Yang, R. Dai, W. Wang, C. Cui, Y. Liang, C. Zhang, C. Li, H. Wang, H. Lu, Z. Yang, H. Zhang, X. Wang, *Phys. Chem. Chem. Phys.*, 2021, **23**, 23173-23183.

5 H. Liu, C. Li, H. P. Zhang, L. J. Fu, Y. P. Wu, H. Q. Wu, *J. Power Sources,* 2006, **159**, 717-720.

6 Q.Liu, G. Tan, P. Wang, S. C. Abeyweera, D. Zhang, Y. Rong, Y. A. Wu, J. Lu, C.-J. Sun, Y. Ren, Y. Liu, R. T. Muehleisen, L. B. Guzowski, J. Li, X. Xiao, Y. Sun, *Nano Energy*, 2017, **36**, 197-205.

7 M. M. Thackeray, *J. Electrochem. Soc.*, 1995, **142**, 2558-2563.

8 P. C. Tsai, W. D. Hsu, S. K. Lin, *J. Electrochem. Soc.*, 2014, **161**, A439.

9 M. Winter, J. O. Besenhard, M. E. Spahr, P. Novák, *Adv. Mater.*, 1998, **10**, 725-763.

10 X. Zhang, V. Aravindan, P. S. Kumar, H. Liu, J. Sundaramurthy, S. Ramakrishna, S. Madhavi, *Nanoscale* 2013, **5**, 5973-5980.